

Maleimides as electron-transfer photoinitiators: quantum yields of triplet states and radical-ion formation

Justus von Sonntag*, Wolfgang Knolle

Institut für Oberflächenmodifizierung IOM e.V., Permoserstraße 15, 04318 Leipzig, Germany

Received 23 May 2000; accepted 31 May 2000

Abstract

The knowledge of quantum yields of triplet states and, moreover, of initiating radicals is a crucial prerequisite to evaluate any novel photoinitiator system. This work provides triplet quantum yields of *N*-methylmaleimide (0.03 ± 0.01), *N*-ethylmaleimide (0.07 ± 0.01) and *N*-propylmaleimide (0.05 ± 0.02) determined by relative actinometry using laser flash photolysis and acetone sensitisation. Unsubstituted maleimide on the other hand shows rapid triplet state tautomerisation, not allowing the application of relative actinometry with triplet sensitisation. The triplet quantum yield was then determined by comparing the transient conductivity of the enolate formed with conductivity actinometry; it is unity.

The yield of initiating radicals is only a fraction of the triplet yield, as the electron transfer reaction includes an efficient back donation. The radical ion yields measured span from 2% (thiocyanate) to 28% (allylthiourea) of the triplet quantum yield. © 2000 Elsevier Science S.A. All rights reserved.

Keywords: Electron transfer; Quantum yield; Photoinitiator; Maleimide: CAS [541-59-3]; Laser flash photolysis; Actinometry; Conductivity detection

1. Introduction

Photoinduced polymer synthesis is a continuously growing field demanding special photoinitiators for use in areas such as outdoor or food package application. The formulations applied in these areas should result in migratable-free coatings with no residual photoinitiator present. Maleimide derivatives have aroused considerable interest in this field as they are copolymerisable and self-bleaching photoinitiators [1–7]. In the 1970s thorough investigations into the use of maleimides as radio-sensitisers [8] and model compounds for photoactive biomolecules [9] has provided information about the radical and photochemistry of maleimide derivatives, both by optical [8] and EPR spectroscopy [10,11]. These data can only with caution be applied for different maleimides, as the maleimide chromophore is very sensitive to substitution. This results in a strong influence of the substituent on triplet quantum yield (see below). The addition of a maleimide end-group to a photoactive molecule also often leads to a photochemistry differing appreciably from its parent compound [7,9,12,13].

A triplet quantum yield close to unity is a prerequisite for any novel photoinitiator system if it is to compete with the established commercial photoinitiators. To our knowledge, the only data available for triplet quantum yields of maleimides is derived from phosphorescence measurements for *N*-butylmaleimide, 0.23–0.24 [9].

While maleimides have been believed for long time to be hydrogen abstracting photoinitiators [1,4,14–17] we have recently shown that they react by electron transfer with unsaturated monomers [5]. The high rate ($>10^9 \text{ s}^{-1}$ in neat resin) of initiating radical formation is, however, accompanied by a low overall quantum yield associated with the electron transfer reaction. While hydrogen back donation does usually not take place, electron back transfer within the radical ion pair is a highly favoured process, especially in apolar solvents. This results in a reduced overall radical ion formation quantum yield. In this paper quantum yields of radical ions of some model systems will be presented. Conventional quantum yield determination by product analysis fails when polymerisable substances are subject to investigation; the high error levels associated with quantum yield determination by laser flash photolysis is, therefore, compensated by the fact that the reference equation is well defined, i.e. consequent (relatively slow) reactions cannot interfere with the determination of the yields.

* Corresponding author. Fax: +49-341-235-2584.
E-mail address: justus@rz.uni-leipzig.de (J.v. Sonntag).

2. Experimental

Maleimide (MI, >98%, Lancaster), *N*-methylmaleimide (MeMI, >99%, Fluka), *N*-ethylmaleimide (EtMI, >98%, Lancaster), *N*-propylmaleimide (ProMI, >98%, Lancaster), 2-nitrobenzaldehyde (ONBA, >99%, Lancaster), benzophenone-4-carboxylic acid (4BC, >99%, Lancaster), thiourea (per synthesis, Merck), allylthiourea (ATU, >98%, Lancaster), *N,N,N',N'*-tetramethylthiourea (per analysis, Fluka), were used as received. Water was purified by a Millipore Milli-Q system. To remove oxygen, samples were purged for at least 7 min with N₂ (5.0, Air Products).

The laser photolysis set-up comprises a 308 nm XeCl-excimer laser (MINex, LTB Berlin, pulse train of three pulses (70, 20 and 10% of total energy, respectively, each with 5 ns half width, all three within 70 ns, total pulse train energy up to 15 mJ) as excitation source and a pulsed xenon short-arc lamp (XBO 450, Osram, power supply LPS 1200, lamp pulser MCP 2010, both Photon Technology International) supplying the analysing-light. The transient recording electronics, a photomultiplier (1P28, Hamamatsu, operated at 900 V, power supply: PS310, Stanford Research Systems) and a 500 MHz, 2.5 GS/s digitising storage oscilloscope (TDS620b, Tektronix) guarantees a time resolution within the limits set by the excitation source. Further details have been published recently [18].

The conductivity detection system consist of a custom made quartz cuvette (quadratic cross-section: 5 mm × 5 mm) with three glassy carbon electrodes (Ø=3 mm) [19,20] and a 50 V, 1 ms DC pulse generator (HP 214 A, Hewlett Packard). The voltage drop over a 50 Ω resistor is amplified 10-fold by a custom made 400 MHz-to-DC amplifier (on basis of a Burr-Brown OPA 687).

A laser pulse energy monitoring system [21] allows us to correct for the short-term energy variation of the laser employed.

2.1. Actinometry

Optical actinometry was performed based on the transient absorbance of the 4-carboxylate benzophenone triplet (³4BC⁻) at 340 nm ($\epsilon=880 \text{ m}^2 \text{ mol}^{-1}$, triplet quantum yield $\Phi_T=1$) [22]. The influence of ground state absorbance on the observed 'signal' concentration Δc_s was modelled according to Eq. (1). (With E being the negative ground state absorbance to the base of e , d the diameter of the analysing-light pinhole in the cuvette screen, x_S and x_E the distances of the beginning and end of the pinhole measured from the laser-side cuvette wall, respectively. I_0 and Φ denote the laser light intensity and the triplet quantum yield, respectively.) The derivation of Eq. (1) has been published recently [18].

$$\Delta \bar{c}_s = -I_0 \Phi \frac{\pi}{d^2} \frac{E}{E^2 + (\pi/d)^2} (\exp(Ex_E) + \exp(Ex_S)) \quad (1)$$

The conductometric detection was calibrated with the 2-nitrobenzaldehyde actinometer system (formation of 2-nitrosobenzoic acid with a quantum yield of 0.5) [23]. The ground state absorbance-to-signal ratio of conductometric detection does not follow the same laws as the optical case because electrical field potentials follow curved lines and the geometry of the cuvette with its electrodes is quite complex. Therefore, an empirical formula was used, based on a gamma-distribution function [24]. The observed (geometrically averaged) transient conductivity (Δx) is thus described as a function of the decadic ground state absorbance A , the proportionality factor a and some fitted constants [25].

$$\Delta \bar{x} = I_0 a \exp\left(-\left(\frac{A - 0.98}{2.87}\right)\right) \left(\frac{A - 0.98}{0.92} - 7.3\right)^{0.32} \quad (2)$$

Transient conductivity detection is very well suited for quantitative determination of quantum yields, because the specific conductivity of transients can easily be estimated from their structure [26]. In the case described in the following produces the actinometry system used (an organic acid anion plus a proton) within some percent error the same specific conductivity as the investigated transient pair (another organic acid anion plus a proton). The specific conductivity of the proton is known, $350 \times 10^{-4} \text{ m}^2 \text{ S mol}^{-1}$ [27] and accounts anyway for most of the total conductivity. The specific conductivity of the anion can furthermore be estimated with sufficient accuracy to $33 \pm 10 \times 10^{-4} \text{ m}^2 \text{ S mol}^{-1}$ [27].

2.2. Pulse radiolysis

The pulse radiolysis set-up uses an 11 MeV-linear accelerator (Elektronika U 003, Thorium, Moscow, Russia, 5 ns, 17 Gy) and an optical detection system similar to that of the laser flash photolysis set-up. Details have been published elsewhere [28]. The dose was determined by thiocyanate dosimetry [29].

The absorption coefficients of the *N*-alkylmaleimide radical anions were determined 10 μs after the pulse (5 ns, 17 Gy, 1 mmol dm⁻³ (*N*-alkyl-) maleimide, 0.5 mol dm⁻³ *t*-butanol, nitrogen purged). The spectra were corrected for the hydrogen adduct spectrum obtained by pulse radiolysis of the same solution saturated with N₂O.

3. Results and discussion

3.1. *N*-alkylmaleimides

The determination of triplet quantum yields of the *N*-alkylmaleimides has been performed by relative actinometry [30]. Acetone (1.0 mass%=0.17 mol dm⁻³ in water) has been used to sensitise the *N*-alkylmaleimide triplet states. The absolute absorbance coefficients of the *N*-alkylmaleimide triplet states were determined by comparing the maximum yield obtained with the initial yield

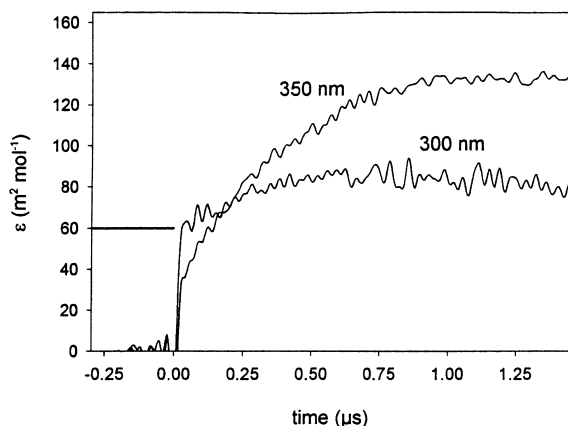


Fig. 1. Determination of absorbance coefficients by triplet sensitisation. The initial acetone triplet concentration is determined at 300 nm ($60 \text{ m}^2 \text{ mol}^{-1}$); the spectrum of the energy acceptor (*N*-alkylmaleimide) triplet state at the time of total conversion ($1 \mu\text{s}$) is then divided by this concentration. Experimental conditions: 1.0 mass% (0.17 mol dm^{-3}) acetone in water, $2.4 \times 10^{-4} \text{ mol dm}^{-3}$ *N*-methylmaleimide, nitrogen purged, data Fourier-filtered.

of acetone triplet ($60 \text{ m}^2 \text{ mol}^{-1}$ at 300 nm, [30]), shown in Fig. 1.

The energy transfer was taken to be quantitative. The rate of energy transfer was found to be diffusion controlled ($>10^{10} \text{ dm}^3 \text{ mol}^{-1} \text{ s}^{-1}$), supporting the assumption of quantitative energy transfer [31]. The acetone-sensitised *N*-alkylmaleimide triplet spectra are shown in Fig. 2.

The spectra obtained by direct excitation (Fig. 3) were compared with actinometry [18] taking the differences in ground state absorbances (cf Eq. (1)) into account. This gives the products of quantum yield and absorbance coefficient for each *N*-alkylmaleimide and wavelength. It is apparent from Figs. 2 and 3 that the spectra observed are reasonably identical in maximum and shape (acetone cuts off wave-

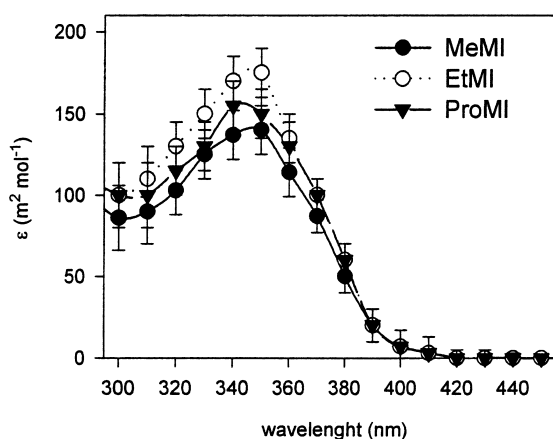


Fig. 2. Acetone-triplet-sensitised spectra of *N*-alkylmaleimides at temporal maximum of the transient. Experimental conditions: 1.0 mass% acetone in aqueous *N*-alkylmaleimide solution (concentrations: $2.4 \times 10^{-4} \text{ mol dm}^{-3}$ MeMI, $2.7 \times 10^{-4} \text{ mol dm}^{-3}$ EtMI, $2.9 \times 10^{-4} \text{ mol dm}^{-3}$ ProMI, respectively).

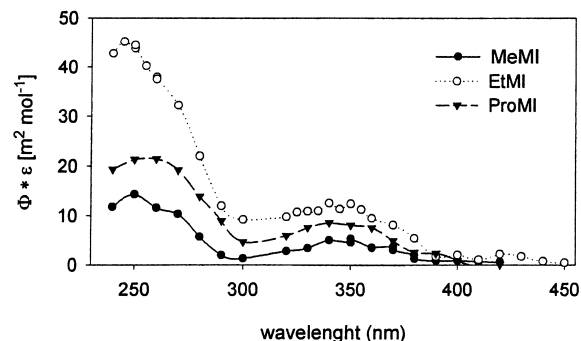


Fig. 3. Direct excitation spectra of *N*-alkylmaleimides in aqueous solution. Experimental conditions (in all three cases): 1.0 mmol dm^{-3} *N*-alkylmaleimide, nitrogen purged. Absolute quantum yield: absorbance coefficient products ($\Phi\epsilon$) obtained by comparison with actinometry [18].

lengths below 300 nm). Dividing the direct excitation quantum yield times absorbance by the sensitised absorbance gives the quantum yield of intersystem crossing for each maleimide investigated. The values are compiled in Table 1.

3.2. Unsubstituted maleimide

Unsubstituted maleimide shows triplet state tautomerisation (and subsequent enol deprotonation) leading to complex spectra and time profiles which do not allow the determination of triplet quantum yield in the same straightforward way as with the *N*-alkylmaleimides [6,25].

Ground state maleimide exists exclusively in the keto form [6]. Upon excitation and intersystem crossing the keto form of the triplet is formed. This transforms into the enol tautomer (reaction (3), $k=5 \times 10^6 \text{ s}^{-1}$, [25]) which subsequently deprotonates (reaction (4), $k \approx 9 \times 10^6 \text{ s}^{-1}$, [25]). The enol triplet is a fairly strong acid with a $\text{p}K_{\text{a}}$ of 3.55 [25].

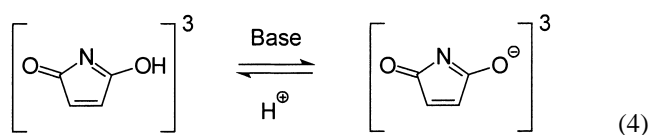
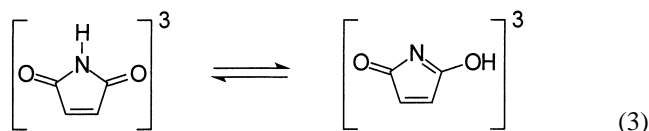


Table 1
Triplet-triplet absorption coefficients at 350 nm and triplet quantum yields (Φ_{T}) of *N*-alkylmaleimides upon direct excitation at 308 nm

Compound	ϵ sensitised ($\text{m}^2 \text{ mol}^{-1}$)	$\Phi_{\text{T}}\epsilon$ by direct excitation ($\text{m}^2 \text{ mol}^{-1}$)	Φ_{T}
<i>N</i> -methylmaleimide	140 ± 15	4 ± 1	0.03 ± 0.01
<i>N</i> -ethylmaleimide	175 ± 15	12 ± 2	0.07 ± 0.01
<i>N</i> -propylmaleimide	155 ± 15	8 ± 2	0.05 ± 0.02

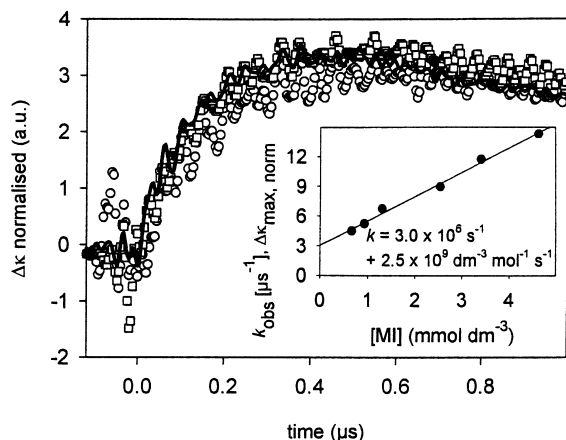


Fig. 4. Transient conductivity at three different doses, normalised to dose [18]. Experimental conditions: $1.30 \text{ mmol dm}^{-3}$ aqueous maleimide, nitrogen purged, Fourier-filtered to 50 MHz bandwidth. (—): full intensity laser beam, (□): half intensity laser beam, (○): quarter intensity. In the inset: observed rate of conductivity build-up vs. maleimide concentration.

This excited enolate acid decays again quickly by unimolecular triplet decay (around $1 \times 10^6 \text{ s}^{-1}$, denoted by 'ISC' as index) and by triplet state quenching, for example, by ground state maleimide (around $2 \times 10^9 \text{ dm}^3 \text{ mol}^{-1} \text{ s}^{-1}$) [5]. These processes compete also for the keto form of the triplet, leading to a decreased yield of conductivity with decreasing triplet lifetime, i.e. increasing maleimide concentration (Fig. 4).

A comparison of the yield of conductivity of the actinometer system and directly excited maleimide is shown in Fig. 5.

Fitting the data obtained with a competition Eq. (5) results in two constants, the maximum yield ($\Phi_{\text{deprotonation}}$, which is found to be approximately unity) and the rate of 'escape' from quenching, i.e. the convolution product of the rate of tautomerisation and subsequent deprotonation, $3.0 \pm 0.2 \times 10^6 \text{ s}^{-1}$. This value is in agreement with the intercept in the inset in Fig. 4. The quantum yield of radical ions $\Phi_{\text{radical ions}}$ as product of the self-quenching (index: 'sq') [5]

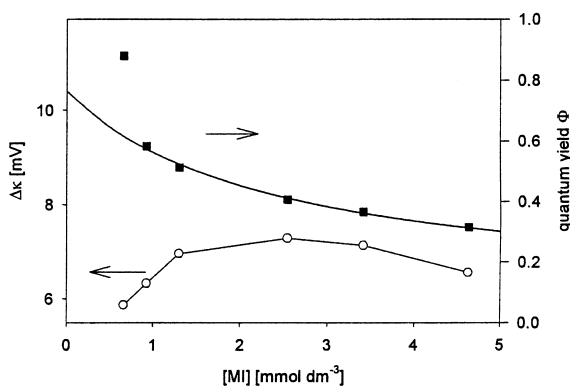


Fig. 5. Quantum yield of enolate deprotonation. (○): measured yield of conductivity at temporal maximum, (■): quantum yield, (—): fit function (Eq. (5)).

is discussed later.

$$\Phi = \frac{k_{3+4}\Phi_{\text{deprotonation}} + k_{\text{sq}}[\text{MI}]\Phi_{\text{radical ions}}}{k_{3+4} + k_{\text{ISC}} + k_{\text{sq}}[\text{MI}]} \quad (5)$$

3.3. Formation of radical ions

Triplet state quantum yields only give an upper limit to the initiation quantum yields. In theory, two initiating radicals can be formed from one triplet state. Usually, however, one of the radicals formed does not initiate polymerisation (as is also the case with maleimides [6]). Triplet state quenching by oxygen and monomers, unimolecular triplet decay and so on further reduce the yield of initiating radicals. Electron transfer processes (as operative with maleimides) can be especially inefficient due to a fast back electron transfer [31].

Radical ion yields were mainly determined for unsubstituted maleimide, the triplet quantum yield of the *N*-alkylmaleimides being so low (<0.1) that the radical ion yields are scarcely accessible experimentally.

First the maleimide triplet absorbance coefficients (Fig. 6) were determined by relative actinometry [18,30] using a quantum yield of unity (see above). From then on, the initial absorbance of the maleimide triplet was used to determine triplet concentrations.

As a rule of thumb radical cations are very short-lived and do not exhibit characteristic transient spectra. There are fortunately some possibilities to circumvent this rule. One probe for one-electron oxidation is formed by the pseudohalogenides (Cl^- , Br^- , I^- , SCN^-). They form radicals upon photooxidation and subsequently dimerise rapidly to the well-known dimer radical anions [32]. An example ($\text{Br}_2^{\bullet-}$) is shown in Fig. 7. The absorption coefficient of the thiocyanate radical anion dimer is high enough to produce an observable spectrum even in the case of *N*-ethylmaleimide,

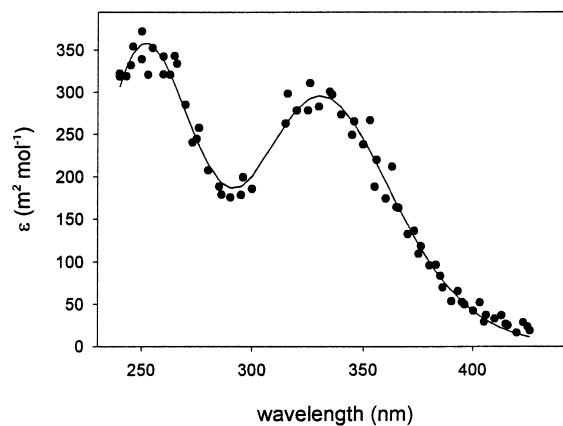


Fig. 6. Triplet-triplet absorbance coefficients of keto maleimide (50 ns after beginning of the laser pulse) in deaerated aqueous solution. Experimental conditions: measurements (symbols ●) taken at different maleimide concentrations, corrected for ground state absorbance by Eq. (1). The fit-function (—) consists of the sum of two Gaussian peaks and was fitted in the frequency domain.

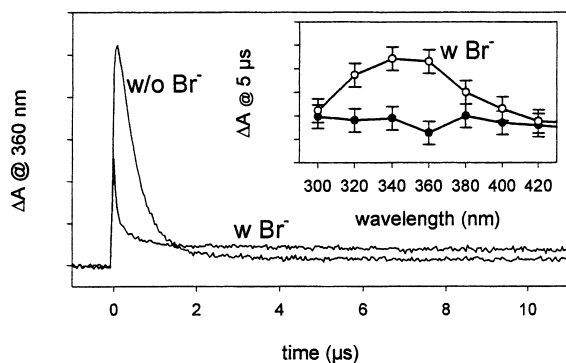


Fig. 7. Time profiles of photoexcited maleimide with and without bromide (potassium salt) added. The lifetime of the triplet state is reduced by the addition of bromide and a long-lived absorbance at 360 nm is formed. This absorbance can be attributed to the bromide dimer radical anion, as shown by the spectrum in the inset. Comparison of the initial maleimide triplet absorbance ($\epsilon_{330\text{nm}}=295\text{ m}^2\text{ mol}^{-1}$, this work) without bromide and the remaining absorbance of $\text{Br}_2^{\bullet-}$ ($\lambda_{\text{max}}=360\text{ nm}$, $\epsilon_{360\text{nm}}=990\text{ m}^2\text{ mol}^{-1}$ [32]) leads to a quantum yield of 0.02 ± 0.01 .

where the overall quantum yield of radical ion formation is only 0.2% ($\sim 2.5\%$ of the triplet quantum yield).

A model system better resembling organic monomers than the pseudohalogenides is thiourea and its derivatives. Thiourea has recently been found to form rather stable radical cations (and subsequently radical cation dimers) with a characteristic and quantitatively determined absorption spectrum (thiourea $\lambda_{\text{max}}=400\text{ nm}$, $\epsilon_{\text{max}}=740\text{ m}^2\text{ mol}^{-1}$, tetramethylthiourea $\lambda_{\text{max}}=450\text{ nm}$, $\epsilon_{\text{max}}=656\text{ m}^2\text{ mol}^{-1}$ [33,34]). Laser flash photolysis of maleimide with addition of thiourea or tetramethylthiourea in aqueous solution produces with high rate constants ($4.8\times 10^9\text{ dm}^3\text{ mol}^{-1}\text{ s}^{-1}$ for thiourea [34], $3.9\times 10^9\text{ dm}^3\text{ mol}^{-1}\text{ s}^{-1}$ for tetramethylthiourea [34], $3.9\times 10^9\text{ dm}^3\text{ mol}^{-1}\text{ s}^{-1}$ for ATU [6]) the spectra expected for the photooxidation of the thiourea derivatives (Fig. 8). A quantitative analysis of the spectra taking into account

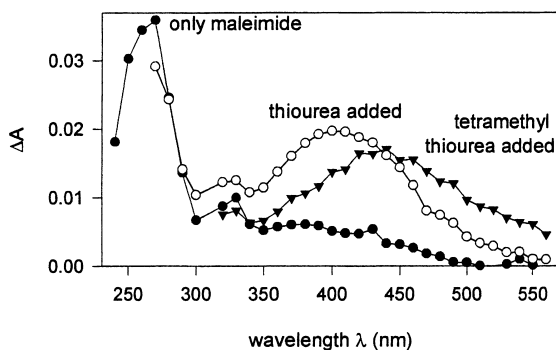


Fig. 8. Transient spectra obtained $3\mu\text{s}$ after the laser pulse. Experimental conditions: 2.5 mmol dm^{-3} aqueous maleimide solution, nitrogen purged. (●): only maleimide; (○): 16.3 mmol dm^{-3} thiourea added; (▼): 16.8 mmol dm^{-3} tetramethylthiourea added. Quantitative analysis leads to quantum yields of 12 and 10% for thiourea and tetramethylthiourea, respectively.

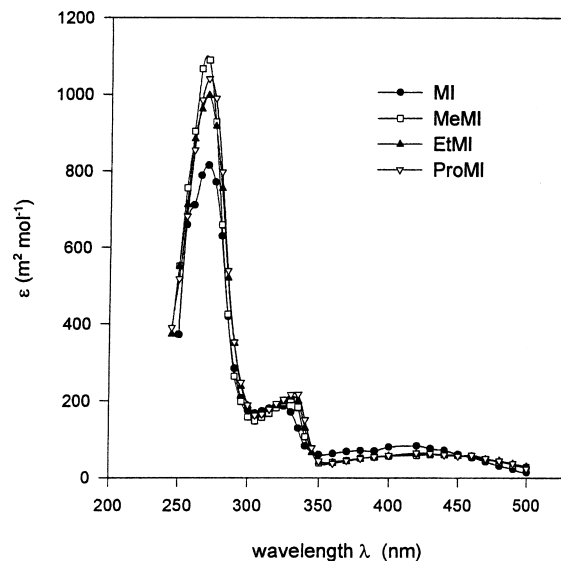


Fig. 9. Quantitative transient spectra of maleimide radical anions. Experimental conditions: 1.0 mmol dm^{-3} (*N*-alkyl-) maleimide, 0.5 mmol dm^{-3} *t*-butanol, nitrogen purged, 17 Gy per pulse.

the initial maleimide triplet concentration determined beforehand leads to radical ion formation (quantum) yields of 12% for thiourea and 10% for tetramethylthiourea.

It is, however, apparent from Fig. 8 that the laser flash photolysis of aqueous maleimide solutions without additional triplet quenchers also leads to a long-lived product. It was identified by EPR [5] to be the rather stable maleimide radical anion. The optical spectrum of the *N*-ethylmaleimide radical anion is known for long, [8], the spectra of the other *N*-alkylmaleimide radical anions and the unsubstituted maleimide radical anion are similar and were obtained by pulse radiolysis (Fig. 9).

The main characteristic absorbance of the maleimide radical anions lies in the UV-C (240–300 nm), a region where the ground state of many monomers has a substantial absorbance, too. This combined with the formation of other poorly defined species (the radical cations of the comonomers, their dimers and adducts onto the (*N*-alkyl-) maleimide) does not allow a quantification of the radical ion yield in the case of the monomers tested (see compilation of rate constants in [5,6]), except for maleimide itself. ATU and its radical cation (and presumably its dimer) do not exhibit any substantial absorbance at 270 nm [35] and furthermore show a relatively large electron transfer yield.



As a consistency check in this case the absorbances at several wavelengths were used and a range of ATU concentrations (and therefore relative triplet quenching capacities) was evaluated according to the competition equations (7) and (8). The competition equation (7) allows to calculate the overall quantum yield (Φ_{ov}) as a function of the quantum yields of the three concurrent reactions involved: triplet

Table 2

Radical ion quantum yields of unsubstituted maleimide (Φ_{RI}) as determined by time-resolved quantitative absorption spectroscopy

Scavenger	Φ_{RI}
Allylthiourea	0.28±0.05
Thiourea	0.12±0.03
Tetramethylthiourea	0.10±0.03
Maleimide itself	0.10±0.05
Thiocyanate (potassium salt)	0.02±0.01
Bromide (potassium salt)	0.02±0.01
Thiocyanate (with <i>N</i> -ethylmaleimide)	0.025±0.01
	$\times \Phi_{\text{T}(N\text{-ethylmaleimide})}$

quenching¹ by ATU, by maleimide (MI) and product-free unimolecular triplet decay by intersystem crossing (ISC).

$$\Phi_{\text{ov}} = \frac{\Phi_{\text{ATU}} k_{\text{ATU}} [\text{ATU}] + \Phi_{\text{MI}} k_{\text{MI}} [\text{MI}]}{k_{\text{ATU}} [\text{ATU}] + k_{\text{MI}} [\text{MI}] + k_{\text{ISC}}} \quad (7)$$

The denominator of Eq. (7) can be summarised as total triplet decay rate (s^{-1}), k_{ov} . Eq. (7) can then be transformed into a linear relationship between the overall quantum yield and the ATU concentration as the maleimide concentration was held constant in this set of experiments. The linear regression function is defined explicitly and does, therefore, not rely on iterations which leads to a far superior reliability of the fit results.

$$\Phi_{\text{ov}} \frac{k_{\text{ov}}}{k_{\text{ATU}}} = \Phi_{\text{ATU}} [\text{ATU}] + \Phi_{\text{MI}} \frac{k_{\text{MI}}}{k_{\text{ATU}}} [\text{MI}] \quad (8)$$

The results of this chapter are collected in Table 2 and Fig. 10. The long-lived transient spectra formed by quenching the maleimide triplet state with other unsaturated monomers (e.g. vinyl ethers, *N*-vinylpyrrolidone, methacrylic acid) indicate quantum yields of radical ion formation in the range from 5% (4-hydroxybutylvinylether, HBVE) to 25% (*N*-vinylpyrrolidone, NVP) [6]. Grishina et al. [36] reported an increase in quantum yield with electron donor strength for a similar system. Qualitatively this is found true for the maleimide-donor system, too (Fig. 10).

3.4. Aromatic maleimides

The simple phenyl maleimide does not show the characteristic triplet spectrum during laser flash photolysis experiments. It also does not photoinitiate free radical polymerisations [6,7]. Sterically hindered aromatic maleimides (e.g. by introduction of bulky *ortho*-substituents) on the other hand do photoinitiate, showing again the strong substitution dependency of the maleimide chromophor [7].

¹ The tautomerisation reaction is believed not to interfere that much in this case, as both tautomers are triplet states showing an almost identical chemistry.

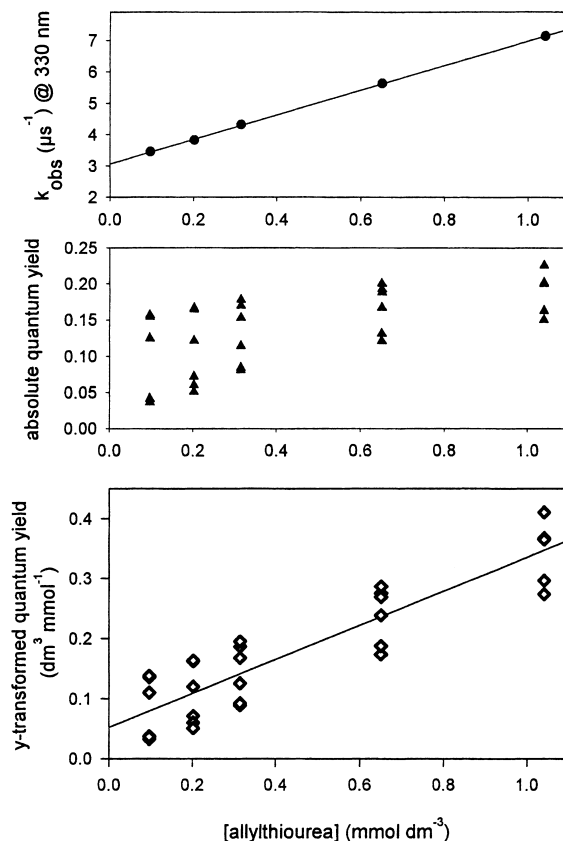


Fig. 10. Determination of radical ion formation quantum yields of the self-quenching and of the quenching by ATU. Top (●): total rate of triplet decay, centre (▲): overall radical ion formation quantum yield determined at different wavelengths, bottom (◇) with (8) transformed overall radical ion formation quantum yield, all three diagrams vs. ATU concentration. Evaluation of the slope and the intercept of the bottom diagram leads to $\Phi_{\text{ATU}}=28\%$ and $\Phi_{\text{MI}}=10\%$.

4. Conclusion

The triplet quantum yields of differently substituted maleimides have been shown to span the range from approximately zero (*N*-phenylmaleimide) over 0.03 (*N*-methylmaleimide), 0.07 (*N*-ethylmaleimide), 0.24 (*N*-butylmaleimide, [9]) to unity (unsubstituted maleimide).

This feature renders mechanistic conclusions based on comparison of the photoinitiating performance of differently substituted maleimides as tried in [1,14,15,37–39] to no avail.

The practical consequence of the data presented here is, that the unsubstituted maleimide should be the best performing photoinitiator in this class, its toxicity and poor solubility, however, does not recommend it for practical applications. The low triplet quantum yields are a major drawback of *N*-alkylmaleimide photoinitiators, but can be overcome by triplet sensitisation with, e.g. benzophenone [40]. This, of course, does not lead to an extractable-free cured product as a truly maleimide photoinitiated coating, but already minute

amounts of maleimides added are reported to improve the benzophenone-amine system to some degree [41,42].

Acknowledgements

The authors wish to acknowledge Prof. Dr. R. Mehnert for continuous support and interest, Dr. I. Janovský for helpful discussions and Mr. M. Krieger for manufacturing the electronics of the conductivity set-up.

References

- [1] S.C. Clark, C.E. Hoyle, S. Jönsson, F. Morel, C. Decker, Photo-initiation Efficiency of *N*-functional Aliphaticmaleimides, Radtech North America, Chicago, 1997.
- [2] H. Aida, I. Takase, M. Kambayashi, Fukui Daigaku Kogakubu Kenkyu Hokoku 33 (1985) 43–49.
- [3] H.-J. Timpe, Topics Curr. Chem. 156 (1990) 167–197.
- [4] K. Viswanathan, S. Clark, C. Miller, C.E. Hoyle, S. Jönsson, L. Shao, Polym. Prepr. 39 (1998) 644–645.
- [5] J. von Sonntag, D. Beckert, W. Knolle, R. Mehnert, Radiat. Phys. Chem. 55 (1999) 609–613.
- [6] J. von Sonntag, Kinetische Untersuchungen zur Photochemie des Maleimids und seiner Derivate, Beiträge zum Mechanismus selbstinitiiertter radikalischer Polymerisationen, Dissertation, Universität Leipzig, 2000.
- [7] S.C. Clark, Photopolymerization and photophysical studies of *N*-aliphaticmaleimides, Dissertation, University of Southern Mississippi, 1998.
- [8] E. Hayon, M. Simic, Radiat. Res. 50 (1972) 464–478.
- [9] J. Put, F.C. De Schryver, J. Am. Chem. Soc. 95 (1973) 137–145.
- [10] P.B. Ayscough, T.H. English, G. Lambert, J. Chem. Soc., Faraday Trans. I 73 (1977) 1302–1310.
- [11] P.B. Ayscough, A.J. Elliot, J. Chem. Soc., Faraday Trans. I 72 (1976) 791–798.
- [12] G. Weidinger, Neue photoinitiatoren und photoaktive polymere, Dissertation, Technische Universität Wien, 1993.
- [13] J.M. Warman, R. Abellon, H.J. Verhey, J.W. Verhoeven, J.W. Hofstra, J. Phys. Chem. B 101 (1997) 4913–4916.
- [14] C.W. Miller, S. Jönsson, C.E. Hoyle, C. Hasselgren, T. Haraldsson, L. Shao, Photocuring of Acrylic Systems using *N*-arylmaleimides and *N*-alkylmaleimides as Comonomer-photoinitiators, Radtech North America, Chicago, 1998.
- [15] T. Haraldsson, S. Jönsson, L. Carlsson, C. Hasselgren, C. Wiberg, Effects of Hydrogen-abstraction in Photopolymerised Monofunctional Systems, Radtech North America, Chicago, 1997.
- [16] C. Decker, F. Morel, S. Jönsson, S. Clark, C.E. Hoyle, Macromol. Chem. Phys. 200 (1999) 1005–1013.
- [17] A. Lund, P.O. Samskog, J. Phys. Chem. 86 (1982) 2458–2462.
- [18] J. von Sonntag, J. Photochem. Photobiol. A: Chem. 126 (1999) 1–5.
- [19] R. Dübgen, G. Popp, Z. Werkstoff. 15 (1984) 331–338.
- [20] W.E. van der Linden, J.W. Dieker, Anal. Chim. Acta 119 (1980) 1–7.
- [21] J. von Sonntag, W. Knolle, J. Photochem. Photobiol. A: Chem. 132 (2000) 25–27.
- [22] J.K. Hurley, H. Linschitz, A.J. Treinin, J. Phys. Chem. 92 (1988) 5151–5159.
- [23] R.G.E. Morales, G.P. Jara, Limnol. Oceanogr. 38 (1993) 703–705.
- [24] AISN Software Inc., TableCurve2D Automated Curve Fitting Software User's Manual, Jandel Corporation, San Rafael, 1994.
- [25] J. von Sonntag, W. Knolle, R. Mehnert, in preparation.
- [26] M. von Raumer, A. Sarbach, E. Haselbach, J. Photochem. Photobiol. A: Chem. 121 (1999) 75–82.
- [27] G.R. Dey, D.B. Naik, K. Kishore, P.N. Moorthy, J. Chem. Soc., Perkin Trans. 2 (1994) 1625–1629.
- [28] W. Knolle, R. Mehnert, Nucl. Instr. Methods B 105 (1995) 154–158.
- [29] G.V. Buxton, C.R. Stuart, J. Chem. Soc., Faraday Trans. 91 (1995) 279–281.
- [30] I. Carmichael, G.L. Hug, J. Phys. Chem. Ref. Data 15 (1986) 1–250.
- [31] Autorenkollektiv, Einführung in die Photochemie, VEB Deutscher Verlag der Wissenschaften, Berlin, 1976.
- [32] G.L. Hug, Optical Spectra of Nonmetallic Inorganic Transient Species in Aqueous Solution, US Government Printing Office, Washington, DC, 1981.
- [33] W.-F. Wang, M.N. Schuchmann, H.-P. Schuchmann, W. Knolle, J. von Sonntag, C. von Sonntag, J. Am. Chem. Soc. 121 (1999) 238–245.
- [34] M.N. Schuchmann, H.-P. Schuchmann, W. Knolle, J. von Sonntag, S. Naumov, W.-F. Wang, C. von Sonntag, Nukleonika, 2000, in press.
- [35] K. Vacek, J. Geimer, D. Beckert, R. Mehnert, J. Chem. Soc., Perkin Trans. 2 (1999) 2469–2471.
- [36] A.D. Grishina, A.V. Vannikov, G.O. Khazova, M.G. Teodoradze, Y.I. Koltsov, J. Photochem. Photobiol. A: Chem. 114 (1998) 159–162.
- [37] C.E. Hoyle, S.C. Clark, S. Jönsson, M. Shimose, Polymer 38 (1997) 5695–5697.
- [38] S.C. Clark, C.E. Hoyle, S. Jönsson, F. Morel, C. Decker, Polymer 40 (1999) 5063–5072.
- [39] S. Jönsson, K. Viswanathan, C.E. Hoyle, S.C. Clark, C. Miller, F. Morel, C. Decker, Acceptor Monomers as Efficient Hydrogen Abstracting Photoinitiators, Radtech Europe, Berlin, 1999.
- [40] C.E. Hoyle, K. Viswanathan, S.C. Clark, C.W. Miller, C. Nguyen, S. Jönsson, L. Shao, Macromolecules 32 (1999) 2793–2795.
- [41] R. Nagarajan, H. Cui, W. Xia, D. Hill, C. Miller, S. Jönsson, C.E. Hoyle, Further Studies on Photoinitiator Blends, Radtech Europe, Berlin, 1999.
- [42] C.E. Hoyle, C. Nguyen, A. Johnson, S.C. Clark, K. Viswanathan, C. Miller, S. Jönsson, D. Hill, W. Zhao, L. Shao, Sensitized Photopolymerization of Maleimide/acrylate Systems, Radtech Europe, Berlin, 1999.